




Strategic assessment of groundwater potential zones: a hybrid geospatial approach

Hamid Nazaripour¹ · Mahdi Sedaghat² · Vahid Shafae³ · Majid Movahedi Rad³ 

Received: 20 March 2024 / Accepted: 17 July 2024 / Published online: 31 July 2024
© The Author(s) 2024

Abstract

Groundwater aquifers constitute the primary water supply for populations in arid regions, exemplified by the Goharkooh Plain in Iran's driest drainage basin, where conditions of high evapotranspiration and low precipitation prevail. With the escalating demand for water resources, driven mainly by agricultural expansion, the strategic management of groundwater assets has become increasingly critical. This study focuses on delineating groundwater potential zones (GWPZs) through an integrated approach combining multi-criteria decision analysis and geospatial tools. Based on an extensive literature review, nine thematic layers were selected and developed: lithology, geology, drainage density, slope gradient, elevation, vegetation cover, lineament density, land use, and precipitation. These criteria were initially weighted using the analytical hierarchical process (AHP) and subsequently integrated via weighted overlay analysis. In this research, the strategic selection of thematic layers for assessing groundwater potential in arid regions has been identified as an innovative approach that could significantly advance studies in similar settings. The analysis revealed that approximately 60% of the study area, primarily in the southwestern parts, exhibited moderate to very high groundwater potential. This potential is primarily attributed to the presence of alluvial deposits, low drainage density, and favorable slope and elevation conditions. Applying the receiver operating characteristic (ROC) curve yields an area under the curve (AUC) of 81.5%, indicating a relatively high level of predictive accuracy. These findings demonstrate the efficacy of this integrated approach, suggesting its broader applicability in regions with analogous groundwater challenges and management needs.

Keywords Groundwater potential · MCDM · RS · Drainage density · Weighted overlay analysis

Introduction

Water, as a fundamental natural resource, is pivotal in sustaining human life, driving socioeconomic development, and preserving ecological systems (Makonyo and Msabi 2021). Presently, water resources worldwide are experiencing substantial stress, attributable to the combined impacts of climatic variability and anthropogenic activities. Factors such as burgeoning population growth, accelerated urbanization, industrial expansion, and intensified agricultural practices

have significantly elevated the demand for water (Ghosh et al. 2022). This has led to approximately 57% of the water required for domestic, agricultural, and industrial purposes in arid and semiarid regions, such as Iran, being sourced from groundwater reserves. In certain areas, the dependency on groundwater for drinking water escalates to as high as 65%, presenting considerable challenges in its sustainable utilization. Concurrently, the global status of groundwater resources is witnessing a decline, in terms of both quantity and quality, primarily due to excessive extraction. This over-extraction is leading to lower water table levels, and the insufficiency of surface water in these regions is further exacerbating water scarcity issues (Arulbalaji et al. 2019). The escalation of groundwater exploitation in arid regions is projected to lead to the utilization of fossil water reserves in the future, a practice that is inherently unsustainable (Scanlon et al. 2006).

In light of the scarcity of surface water resources in many regions of Iran, particularly in arid and semiarid

✉ Majid Movahedi Rad
majidmr@sze.hu

¹ Department of Physical Geography, University of Sistan and Baluchestan, Zahedan, Iran

² Department of Geography, Faculty of Social Sciences, Payame Noor University, Tehran, Iran

³ Department of Structural and Geotechnical Engineering, Széchenyi István University, Győr 9026, Hungary

areas, groundwater emerges as the most viable resource for fulfilling water requirements (Madani 2014; Haji Mohammadi et al. 2024). Groundwater is highly prized in arid and semiarid regions not only for its relative freshness and more stable chemical composition, but also for its lower susceptibility to contamination and higher reliability as a water source. Concurrently, it exerts a substantial influence on the ecological capacity of the land, playing an integral role in economic development, ecological diversity, and the health of communities (Izady et al. 2012). The pronounced scarcity and depletion of groundwater in the plains of Iran have escalated into a critical and acute crisis (Bagheri and Hosseini 2011). Aquifers are encountering formidable challenges in the realm of sustainable development, primarily due to declining water levels, deterioration in water quality, increased vulnerability to climate change as a consequence of global warming, alterations in precipitation patterns, and the frequent occurrence of droughts (Foltz 2002; Haji Mohammadi et al. 2024).

The Goharkooh Plain in southeastern Iran represents a region with significant agricultural and tourism development potential within an arid landscape. Here, groundwater serves as the sole source for domestic, agricultural, and industrial needs. The region is currently grappling with an intensified water crisis spurred by a steady rise in population and agricultural expansion, which has drastically heightened water demand (Rezaei and Sargezi 2010). Addressing this crisis necessitates a concentrated effort to effectively manage water consumption, with a particular focus on identifying and managing the aquifer's water potential.

A critical aspect of this endeavor involves the selection of thematic layers, a process fundamental to delineating groundwater resources yet fraught with challenges, particularly in terms of quantity and type. The suitability of these layers is profoundly influenced by the climatic conditions of the study area, necessitating a nuanced approach, in such a way that the thematic layers effective in delineating groundwater resources in an arid environment with scant rainfall and sparse vegetation cover (Elewa and Qaddah 2011; Mallick et al. 2019; Mumtaz et al. 2019) are completely different from those in a temperate mountainous environment with abundant snowfall and dense forest cover (Sapkota et al. 2021). Consequently, the reliability of groundwater potential research hinges on the precise and intelligent selection of factors affecting the groundwater resources of each region. On the other hand, the involvement of numerous thematic layers (Ozdemir 2011) as opposed to effective layers (Khan et al. 2022) can complicate the analysis process and the interpretation of results. In the context of the Goharkooh Plain's dependence on groundwater, it is critical to examine the factors influencing its availability and dynamics. Groundwater potential is shaped by a variety of factors, including physiography, geology, hydrology, land use,

land cover, and climatic elements like precipitation, temperature, and evaporation (Asgher et al. 2022; Ifediegwu 2022). The complexity and variability of these factors can lead to significant changes in groundwater potential within short distances (Dar et al. 2010; Thapa et al. 2017). Despite the region's rich groundwater resources, there is a notable lack of comprehensive studies on its potential zones and the factors that influence them. This gap in knowledge has led to unstructured and excessive exploitation of the groundwater resources, resulting in adverse effects such as land subsidence, changes in land use, and restrictions on water usage. Our research aims to address this gap by employing a meticulous approach to selecting thematic layers, thereby enhancing the reliability of groundwater potential assessments in arid environments such as the Goharkooh Plain.

Systematic data integration in hydrogeological research facilitates the rapid and cost-effective identification of potential groundwater areas, offering a significant advancement over traditional, more time-consuming, and expensive methods such as geophysical and hydrogeological surveys, outcrop mapping, and well drilling (Jha et al. 2010; Barik et al. 2017). Building upon this advancement, remote sensing (RS) technologies and geographical information systems (GIS) emerge as powerful tools for assessing natural resources. They provide high efficiency, low cost, and the capability for complex spatial and spatiotemporal data analyses across extensive areas in a relatively short time frame, presenting a stark contrast to the more traditional methods (Souissi et al. 2018). Over the past decade, researchers have employed various variables and numerous statistical techniques with differing accuracies to delineate the boundaries of groundwater potential. These methods encompass a range of approaches, including the weight of evidence model (Tahmassebpour et al. 2016), the probabilistic frequency ratio model (Manap et al. 2014; Davoodi Moghaddam et al. 2015), the certainty factor (Nampak et al. 2014), gamma fuzzy (Antonakos et al. 2014), Shannon entropy (Naghbi et al. 2015), and multi-criteria decision analysis (Singh et al. 2018; Sandoval and Tiburan Jr. 2019; Brito et al. 2020). Furthermore, machine learning techniques such as random forest (Golkarian et al. 2018; Prasad et al. 2020), artificial neural networks (Lee et al. 2012; Li et al. 2019), logistic regression methods (Chen et al. 2018), and machine learning ensembles (Kamali Maskooni et al. 2020) have also been notable. Among these diverse techniques, RS and GIS have particularly stood out. Compared to conventional hydrogeological survey methods, they have proved effective in producing quick and cost-effective results (Oh et al. 2011), especially in arid and water-scarce regions with limited data availability. This field has garnered significant interest in recent decades, with numerous researchers utilizing RS and GIS for groundwater resource exploration (Deepa et al. 2016; Chen et al. 2018; Rahman et al. 2022). The absence

of such studies in arid and semiarid regions, particularly in the study area, compelled researchers to employ an integrated approach to delineate zones susceptible to groundwater resources.

This study introduces a groundbreaking methodology in the arid environment of the Goharkooh Plain, where RS technologies, GIS, and multi-criteria decision-making (MCDM) are harmoniously integrated. This methodological innovation establishes a thorough and efficient framework for assessing groundwater potential, with a strong emphasis on the comprehensive evaluation of topological, geological, hydroclimatological, and land cover factors. The primary objective is to effectively utilize this integrated approach to identify and evaluate groundwater potential zones (GWPZs) within the aquifer. By harnessing the collective capabilities of RS, GIS, and MCDM, this research endeavors to overcome the limitations inherent in conventional hydrogeological methods. It is anticipated that this novel approach will significantly bolster sustainable management of aquifer resources, increase per capita income, and enhance groundwater governance in the Goharkooh Plain.

The paper is organized as follows: Sect. "Materials and methods" details the methodology employed in this research, which includes utilizing a four-step method to assess the GWPZs in the Goharkooh Plain. This section covers data collection, developing thematic layers using RS and GIS processing, overlay analysis utilizing the analytical hierarchical process (AHP), and validating and confirming the predicted groundwater potential map. Sect. "Results and discussion" presents the outcomes of our study, encompassing the spatial distribution of thematic layers, the analysis of GWPZs, and the comprehensive validation strategy. Finally, Sect. "Conclusion" provides a concise summary of our findings and their implications.

Materials and methods

Study area

The eastern and central regions of Iran, receiving less than 100 mm of rainfall annually, are characterized as hyper-arid and arid climates (Kaboli et al. 2021). Owing to the scarcity of annual rainfall, its considerable temporal and spatial variability, and elevated evaporation rates, substantial and consistent surface flows are rarely formed in these regions. The existing surface flows that do occur are typically seasonal and unpredictable, rendering them unreliable for sustained exploitation. Consequently, there is an increased reliance on the extraction of groundwater resources. However, it is essential to note that groundwater reserves in these areas are often not abundant, further complicating their utilization (Safdari et al. 2022). The

Goharkooh Plain catchment, located in the southeasternmost part of Iran's Lut Desert, spans from 60 degrees 11 min to 61 degrees 7 min East longitude and from 28 degrees 7 min to 28 degrees 45 min North latitude, as depicted in Fig. 1. This region is characterized by extensive alluvial deposits, which serve as the principal reservoir for groundwater storage, forming the Goharkooh aquifer. The mean elevation of the Goharkooh Plain is estimated to be around 1,350 m above sea level. The total area of the catchment is approximately 2,870 square kilometers, of which about 55 percent consists of low-lying alluvial plains, while the remaining 45 percent is composed of mountainous and highland regions. The Goharkooh aquifer, categorized as a free aquifer, is situated within these alluvial and fan deposits and encompasses an area of about 487 square kilometers (Rezaei and Sargezi 2010). In recent decades, the Goharkooh Plain has experienced a significant decline in groundwater levels, primarily attributed to excessive extraction of groundwater resources. This depletion is further compounded by the expansion of agro-industrial complexes and a series of prolonged droughts.

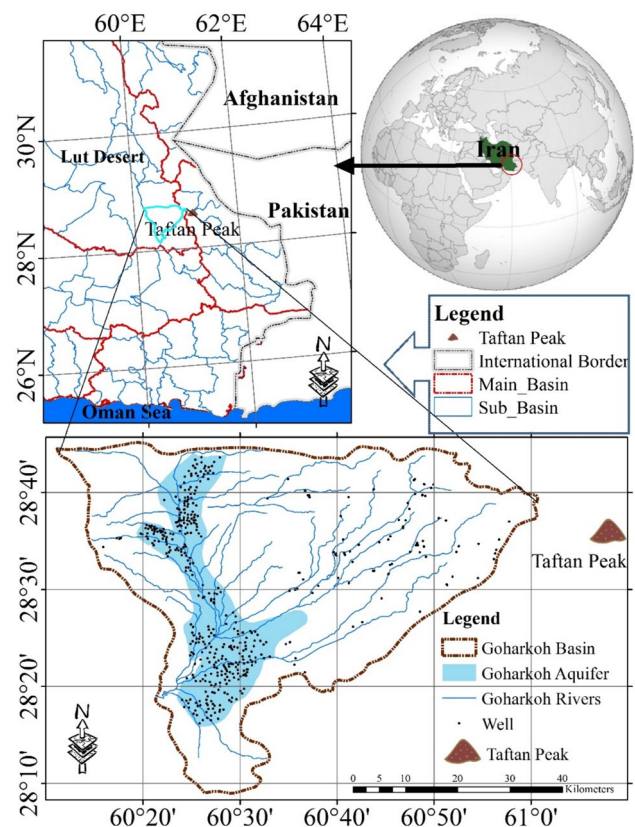


Fig. 1 Drainage and location map of the Goharkooh Plain catchment

Methodology

This study employed a systematic four-step method to assess GWPZs in the Goharkooh Plain. This methodology encompassed: (1) comprehensive data collection, (2) the development of thematic layers through RS and GIS processing, (3) the application of overlay analysis using the AHP for identifying GWPZs, and (4) validation and confirmation of the projected GWPZs map using existing well data from the area. Thematic layers were prepared using RS satellite image data and digitization of existing maps using GIS. Nine critical criteria were considered for evaluating groundwater potential in the study area: lithology, geology, drainage density, slope gradient, digital elevation model (DEM), vegetation cover index, lineament density, land use/land cover (LULC), and annual rainfall. These criteria underwent initial assessment through the AHP method, followed by weight assignment, normalization, and ranking, culminating in a model constructed using a weighted overlay index. Additionally, quantitative validation of the predicted groundwater potential map was conducted employing the receiver operating characteristic (ROC) curve analysis, as illustrated in Fig. 2.

Step 1: data collection

A thorough literature review was conducted to analyze research on the assessment of groundwater potential utilizing GIS and RS methodologies. This review encompassed studies from various regions, including Bangladesh (Adham et al. 2010), Egypt (Abdalla 2012), India (Gupta and Srivastava 2010; Magesh et al. 2012; Mukherjee et al. 2012; Nag

and Ghosh 2013; Selvam et al. 2016; Deepa et al. 2016; Bhave et al. 2019), Iran (Rahmati et al. 2015), South Korea (Lee et al. 2012), Taiwan (Yeh et al. 2016), Thailand (Kaewdum and Chotpantarat 2021), and Sri Lanka (Senanayake et al. 2016). This is aimed at determining the factors that influence groundwater potential. A word cloud visualization (Fig. 3) highlights the significance and frequency of each factor in the modeling of GWPZs based on prior studies. This visual format emphasizes key factors by presenting them in progressively larger font sizes to denote their relative importance. A review of research in the field of GWPZs over the past decade reveals that 18 parameters have been predominantly utilized. The nine most significant parameters—slope, drainage density (DD), LULC, lineament density (LD), soil texture (ST), rainfall, geology, geomorphology, and DEM—have featured in approximately 70% of these studies. Intermediate parameters such as the topographic wetness index (TWI), water table depth (WTD), and lithology have each been employed in 17% of the cases. Additionally, indicators including surface water bodies (SWB), vegetation cover (VC), and surface curvature (SC) have been incorporated in 10% of the studies. More novel parameters, including the topographic position index (TPI), utilized in two instances, and the stream power index (SPI) and hydraulic conductivity (HC), each with a usage rate of 3%, have seen minimal application. These factors, intrinsically tied to the characteristics of aquifers, have been explored and validated in regions bearing similarities to the study area. This methodology is anticipated to enhance the reliability of the GWPZs map.

Consequently, the data compiled for this study encompass a range of biophysical aspects such as slope, drainage

Fig. 2 Methodology flowchart of GWPZs

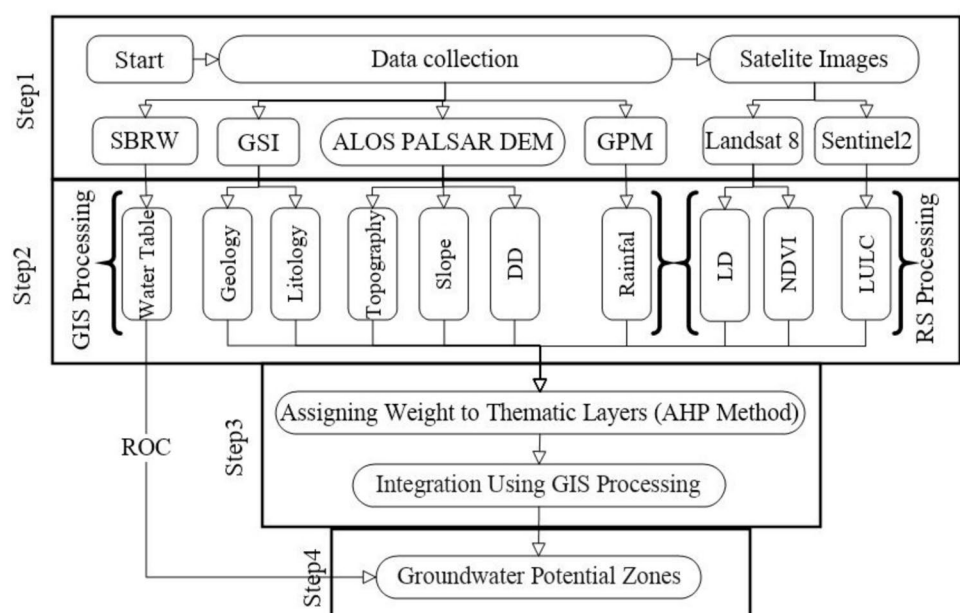


Fig. 3 Word cloud of factors for GWPZs used in the past decade studies



density, LULC, lineament density, rainfall, geology, topography, lithology, and vegetation cover. Additionally, data regarding the location and water level of existing wells in the Goharkooh Plain were also incorporated, with these various datasets being processed to generate thematic layers using diverse geospatial techniques.

Step 2: RS and GIS processing for preparing thematic layers

GIS processing *Geology and Lithology* Geology determines groundwater aquifers. Additionally, the type of rock exposed on the earth's surface, its outcrops, and fractures are directly related to groundwater recharge and feeding (Shaban et al. 2006), resulting in different water bodies in each rock. Groundwater is significantly influenced by various types of rock exposed on the earth's surface (O’Leary et al. 2012).

In studies concerning the potential of water resources, geology investigates the historical alterations in land and soil units over extensive periods. Conversely, lithology focuses on the current physical properties of rock outcrops. Some studies overlook this factor and instead use other physical properties related to secondary porosity, such as lineaments and drainage (Elewa and Qaddah 2011). Here, the geological map and lithological (rock) data are obtained from 1:100,000 scale geological maps of the Geological Survey of Iran (GSI). The characteristics of lithology and geology (age) of the study area are presented in Table 1.

The spatial distribution of geology (Fig. 4A) and lithology (Fig. 4B) shows that, geologically, the Goharkooh Plain watershed is located between the tectonic units of Nehbandan, Khash, Makran, Lut Block, and Central Iran (Aghanabati 2004). The existing rock outcrops in the study

Table 1 Geology and lithology of the study area

Geological Age	Lithological description	Abbreviation code
Quaternary	Current alluvial deposits	Q
	Conglomerate and tuff with andesitic and dacitic components	Qa2
	Old andesitic flow with some basalt	Qan
	Olivine basalt and andesite with conglomerate and interlayers	Qbl
Pliocene	Polymictic conglomerate	PIQ
Miocene	Conglomerate and sandstone with siltstone and some shale	Msc
Oligocene	Granodiorite	gd
Eocene	Shale, limy shale, and limestone	Efv
	Limestone, sandstone, siltstone, shale, and partly limy shale	Efls
	Green to gray sandstone, shale, and some limestone	Es/sh
Paleocene	Mudstone, siltstone, and sandstone, possibly equivalent to the Lut Formation	Ple
Cretaceous	Metamorphosed basic rocks, metamorphosed limy shale, and sandstone	Jk
	Diabase	db
	Gabbro	gb
	Ophiolitic mélange	Cm
Permian	Marble	Pm

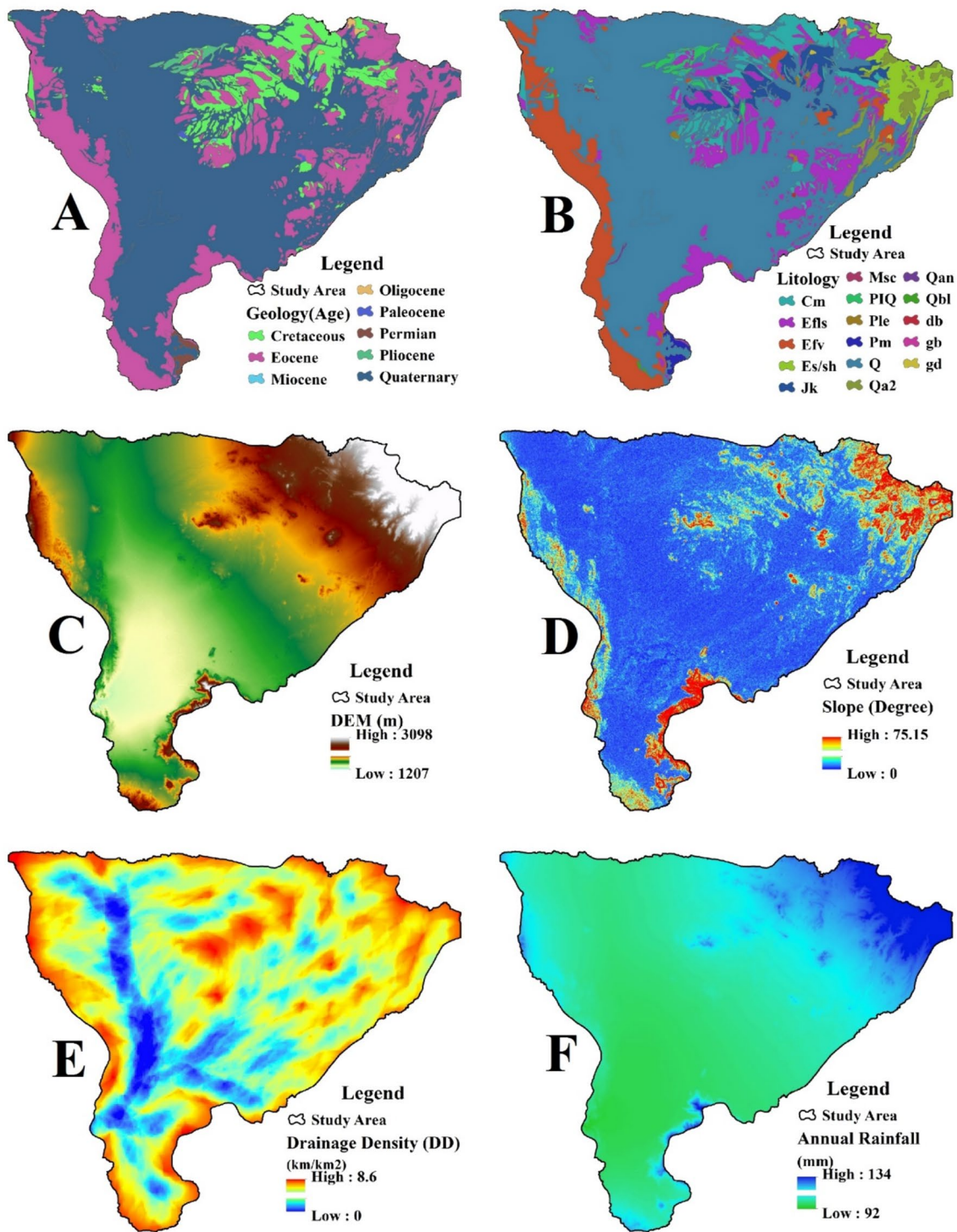


Fig. 4 Thematic layers of parameters: **A** geology; **B** lithology; **C** DEM; **D** slope; **E** drainage density; and **F** rainfall; extracted from GIS processing

area can be structurally divided into two zones: the East Iran Flysch Zone and the Lut Zone associated with Central Iran. The study area consists of flysch deposits and colorful ophiolitic mixtures (Calcolith) of eastern and southeastern

Iran. The major part of the Goharkooh Plain is formed of quaternary alluvial lithology titled current alluvial deposits. Quaternary deposits in the plain include coarse, medium, and fine alluvium. Coarse and medium particles are located

in the central and eastern areas, while fine particles are in the western part of the plain and alluvial fans. These deposits provide a suitable bed for forming and nourishing the aquifer. After that, conglomerate formations have good potential for infiltration, but their spatial extent in the study area is severely limited. Impermeable and hard lithologies are mainly found in the rock outcrops of central and western parts of the study area, which have a low potential for groundwater.

DEM Topographic elevation likely influences the occurrence of groundwater and is regulated by various geomorphological and hydrogeomorphological processes (e.g., geology, meteorological conditions, land degradation, etc.) as outlined by (Pourghasemi and Beheshtirad 2015). Elevation indirectly signifies the role of influential factors on groundwater infiltration, such as slope, drainage network, cumulative flow, and soil. In higher elevations, primarily due to steeper slopes, the infiltration rate of rainwater and surface flows into the subsurface for aquifer recharge and enhancing groundwater potential is minimal. Specifically, in the study area, the minimal vegetation cover in the highlands, which are predominantly covered with hard rock formations, significantly reduces precipitation infiltration. On the other hand, higher elevations are sites of more significant snow and rain accumulation, thereby increasing groundwater recharge potential. Thus, the role of topography is heavily dependent on the geographical and climatic environment of the catchment areas. Due to thermal conditions, snowfall is rare in dry and semiarid regions, especially at lower latitudes.

Consequently, high elevations lacking snow accumulation do not significantly contribute to enhancing groundwater resources. Furthermore, due to steeper slopes, the drainage density is high in higher elevations, and rainwater is quickly converted to surface runoff, draining toward the lower plains and flat areas. The dry geographical environment conditions, along with scant vegetation cover, accelerate this process. Therefore, geographical environments' climatic and biotic conditions in mountainous and rugged areas affect their differing roles in groundwater potential.

The elevation range within the study area varies from 1207 to 3098 m. The average elevation of the study basin is 1350 m, meaning that a substantial portion of the study area is at an elevation lower than 1400 m, primarily encompassing the western part of the study area. Higher elevations are limited to the eastern part, where the dendritic drainage network in the Goharkooh Plain catchment area is formed. The topographic map of the study area (Fig. 4C) has been developed using DEM extracted from ALOS PALSAR RTC data (Laurencelle et al. 2015).

Slope gradient In dry regions characterized by uneven topography, the slope gradient is recognized as a crucial factor influencing groundwater potential. This impact is exerted both directly and indirectly, affecting various elements such

as precipitation, the drainage network, and cumulative flow. It is acknowledged that the infiltration rate of rainfall is predominantly determined by the slope gradient, making it a key factor in these environments (Selvam et al. 2014; Deepa et al. 2016). In areas with gentler slopes, the slower surface flow and increased water accumulation contribute to higher rates of groundwater infiltration. Conversely, the infiltration rate typically decreases in areas characterized by steeper slopes. This is because, on steep slopes, surface waters seldom have the chance to permeate the ground, except in cases where fractures, cracks, and faults provide pathways for infiltration. Furthermore, the slope plays a significant role in shaping the pattern and density of the drainage basin. The slope of the land is also a significant factor in determining groundwater's existence and flow patterns (Yeh et al. 2016).

The thematic slope layer, as depicted in Fig. 4D, was derived from the raster data of DEM, which boasts a resolution of 12.5 m, sourced from ALOS PALSAR. The study area's slope ranges span from a flat zero degrees to a steep 75.15 degrees. Notably, steep slopes are found predominantly in the eastern regions of the study area, particularly in the Tafatan heights, as well as along the eastern and southeastern fringes. Conversely, the slope gradient is relatively gentle in the other parts of the plain. The catchment basin's outlet, located in the southwest corner of the plain, features the minimum slope observed in the study.

Drainage density The drainage network is a highly influential factor in the potential of groundwater, especially in drylands (Yeh et al. 2009). The drainage network reflects the cumulative water flow across the catchment surface and is intricately connected to the process of water infiltration into the subsurface. The density of this network is a critical determinant in ascertaining the potential of areas for groundwater recharge (Yeh et al. 2016). In varying geographical environments, lower-order streams within the drainage network, particularly those of orders 1 and 2, typically exhibit reduced infiltration due to their steeper slopes. In contrast, higher-order streams (orders above 3) demonstrate greater infiltration capabilities. Consequently, the contribution of lower-order streams to overall groundwater replenishment is often considered negligible. As a result, drainage density emerges as a critical factor influencing groundwater potential in dry areas with irregular topography. This density also indirectly reflects the role of precipitation in these environments.

The study area exhibits a dendritic drainage pattern. In such patterns, it is observed that drainage density diminishes in downstream areas as stream orders increase. The drainage density within this area ranges from zero to 8.6 km/km². Notably, areas characterized by low drainage densities are typically flat and plain. This low-density pattern is exemplified by the mainstream flow, which predominantly runs in north–south and east–west directions, as illustrated in Fig. 4E. Thus, according to the

Strahler method (Strahler 1957), streams of orders 1 and 2 are excluded from consideration, focusing the analysis on streams of order 3 and higher for assessing drainage density.

The drainage density length $D_d(\text{km}^{-1})$ is derived from the total drainage length divided by each area unit (Greenbaum 1985) using Eq. (1):

$$D_d = \frac{\sum_{i=1}^{i=n} S_i}{A} \quad (1)$$

In this context, $\sum_{i=1}^{i=n} S_i$ represents the total length of the drainage network within the catchment area (L), while A denotes the unit area (L^2). The total length of the drainage density is closely correlated with the groundwater recharge rate. Specifically, regions exhibiting high drainage density significantly generate surface runoff, resulting in a reduced groundwater recharge volume. To construct the thematic layer representing drainage density, data were utilized from the drainage network ascertained from the DEM in conjunction with the topographic characteristics of the study area.

Precipitation Precipitation, particularly total annual rainfall, is essential for maintaining the hydrological balance within catchment basins and naturally recharging aquifers. Distinct forms of precipitation, including rain and snow, contribute variably to groundwater replenishment. Moreover, the intensity of precipitation profoundly impacts soil water infiltration, a critical process for groundwater recharge. Nonetheless, in small catchments situated in arid and semiarid regions, the negligible spatial variability of precipitation coupled with scant data often complicates the delineation of GWPZs. With the advancement of RS techniques, access to global satellite-based precipitation products like the GPM has improved. The GPM dataset, which spans from 1981 to the present, offers diverse temporal resolutions—daily, pentad, and monthly—and detailed spatial resolutions of 0.25×0.25 and 0.05×0.05 degrees, facilitating an extensive analysis of precipitation on a global scale (Funk et al. 2015). In this study, data with a resolution of 0.05×0.05 degrees were utilized.

In arid regions, exemplified by the Goharkooh Plain catchment, upland areas lack the capacity to sustain aquifers due to sparse vegetation, steep inclines, and low permeability. Conversely, the movement of rainwater from these uplands to lower slopes with reduced flow velocities—particularly in areas with conducive geological conditions—supports the formation of groundwater sources. The spatial distribution of rainfall within this catchment corresponds to its topographical diversity: flat and low-lying areas generally receive minimal precipitation, whereas higher elevations, such as those on the slopes of

Taftan Peak (illustrated in Fig. 4F), record more substantial rainfall. The annual precipitation across the catchment varies from 92 to 134 mm.

RS processes *Vegetation Cover* Vegetation cover, in addition to influencing the infiltration of water into the ground and recharging groundwater aquifers, also prevents surface erosion and, by reducing surface flow, delays the concentration time. The normalized difference vegetation index (NDVI), a RS index, calculates vegetation cover by measuring the difference between the near-infrared spectrum (reflective of vegetation) and the red spectrum (absorptive of vegetation). The NDVI index can be determined from the surface reflectance images of Landsat 8 (L8SR) for identifying green vegetation. The Digital Number (DN) values from L8SR images are converted into reflectance values according to Eq. (2):

$$\text{DN values} + \text{reflectance additive band} \quad (2)$$

Sun angle correction is carried out using Eq. (3):

$$\frac{\text{Reflectance}}{\sin(\text{Sun Elevation})} \quad (3)$$

Subsequently, the vegetation cover index (NDVI) is calculated according to Eq. (4):

$$\text{NDVI} = \frac{(\text{NIR} - \text{Red})}{(\text{NIR} + \text{Red})} \quad (4)$$

Here, NIR refers to the near-infrared band, and Red refers to the red band. NDVI values range from -1 to $+1$, although there is no precise range for a specific phenomenon. However, negative values of this index are likely to include water bodies, clouds, and snow. A range from 0 to 0.4 indicates sparse or no vegetation, while a range above 0.4 represents green and leafy vegetation (Akbar et al. 2019). This index effectively facilitates the extraction of vegetation density maps, land use maps, crop types, plant health, and many other aspects.

In dry and semiarid areas like the Goharkooh basin, natural vegetation is sparse and poor due to limited rainfall. Green vegetation is mainly related to irrigated agriculture on flat lands and gardening along waterways. The range of the vegetation cover index in the study area varies from -0.17 to 0.45 (Fig. 5A). High and very high values of the vegetation index are observed in the lowlands and on alluvial fans dominated by agriculture and gardening. On the other hand, semi-dense vegetation covers, including shrubs and trees, are aligned with gardening uses along waterways.

Lineament Density In a hard rock landscape, lineaments represent fault and fracture zones, leading to increased secondary porosity and permeability (Dinesh Kumar et al. 2007; Selvam et al. 2014). Lineament density is a good

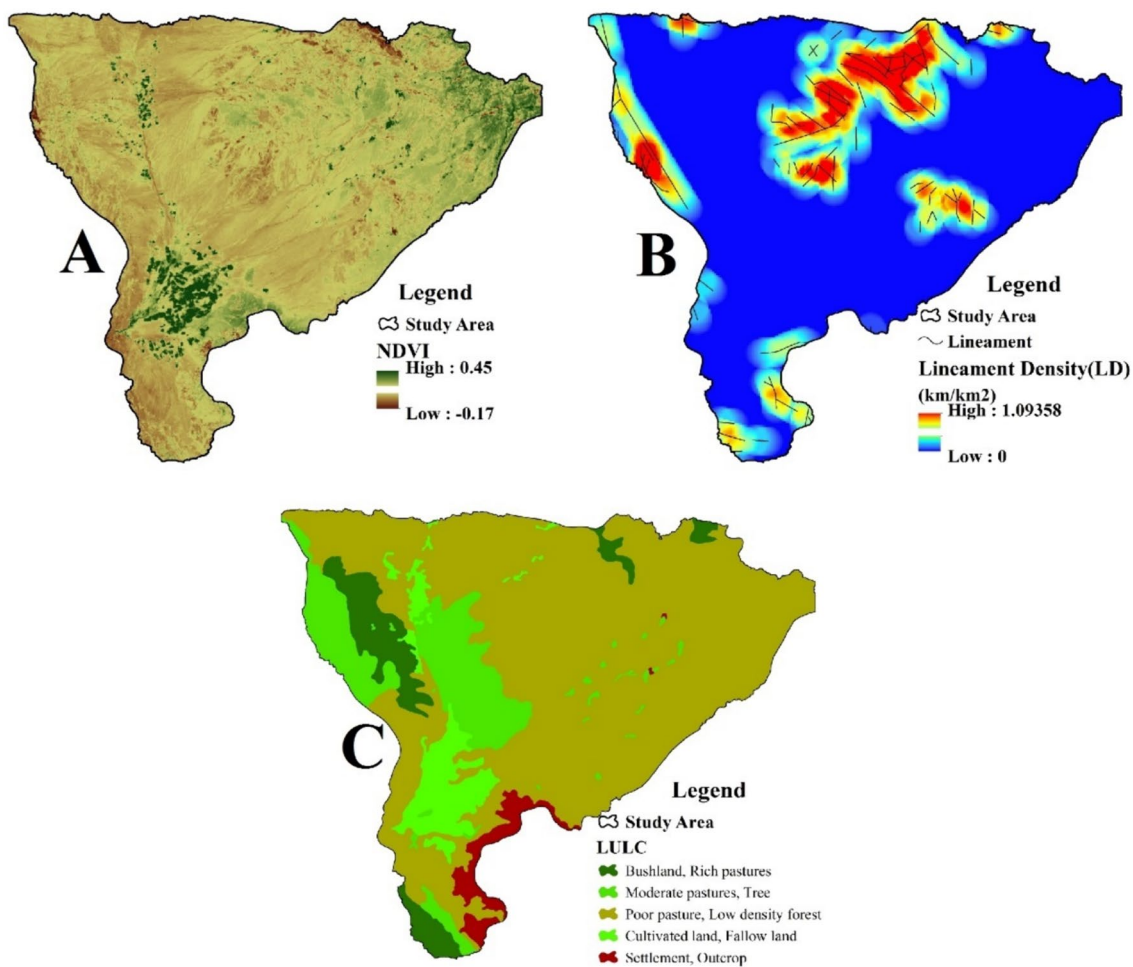


Fig. 5 Thematic layers of parameters: **A** NDVI; **B** LD; **C** LULC; extracted from RS processing

indicator of groundwater recharge, requiring RS analysis of fractures or structures (Yeh et al. 2009). Lineament density L_d (km^{-1}) is derived by dividing the total lineament length by unit area according to Eq. (5):

$$L_d = \frac{\sum_{i=1}^{i=n} L_i}{A} \tag{5}$$

Here, $\sum_{i=1}^{i=n} L_i$ refers to the total lineament length (L) and A refers to the unit area (L^2). High lineament or fracture lengths per unit area indicate a high degree of fracturing and an area with high potential for groundwater recharge. The assessment of lineament density is based on a 1:100,000 scale geological map and a combination of bands 1, 4, and 8 of the Landsat 8 images, using directional filters.

The range of lineament densities in the study area varies from zero to 1.09 km/km^2 (Fig. 5B). The central part of the study area is mainly characterized by hard rock outcrops, which, in addition to weathering, are marked by joints, cracks, fractures, and fault systems. The western regions of

the study area also align with the direction of regional faults. Since a large part of the study area is covered by flat plains with recent alluvial formations, dense lineament areas are limitedly manifested in the central and peripheral regions of the study area.

LULC Land use and land cover are significant factors influencing the recharge of groundwater (Kaewdum and Chotpantararat 2021). Leduc et al. (2001) found that one of the main contributors to groundwater recharge volume is related to changes in land use. Bhave et al. (2019) and Shaban et al. (2006) also concluded that land cover influences groundwater recharge. LULC patterns provide information about infiltration and runoff controlled by the nature of surface materials. LULC data in this study were extracted from six bands of Sentinel-2 surface reflectance data (Karra et al. 2021).

LULC patterns such as cultivated and fallow lands, bushlands and pastures, and scattered trees, poor pastures, settlements, and rocky outcrops exist in the study area (Fig. 5C). In the plain area, the primary land use and cover

are agricultural lands, and in the foothills, there is a dominance of poor pastures and bushlands. In agricultural lands, due to plowing operations, water infiltration is higher. Areas with dense bushlands and rich pastures, characterized by relatively high vegetation density, exhibit significant potential for water infiltration as they effectively reduce surface water flow.

Step 3: weighting the thematic layers using AHP analysis

The AHP is a subset of the MCDM method, involving the analysis and decision-making related to multiple objectives (Cay and Uyan 2013). It is widely used for spatial decision-making in natural resource management, including groundwater issues. AHP is a mental approach where the selection of subclasses and weight allocation are based on comparisons among various criteria derived from appropriate decision strategies. In MCDM analysis, weights are assigned to each influencing factor, considering its role in a specific region (Agarwal and Garg 2016; Jhariya et al. 2017). AHP methodology involves calculating weights from a preference matrix that represents map layers. Weights are created by comparing related criteria based on preferential factors. The ability to handle a large amount of heterogeneous data in a forward and clear manner, based on weights, makes this method one of the most popular approaches in different GIS systems (Feizizadeh and Blaschke 2012; Khan and Jhariya 2019). The inference of weights for the main thematic layers and their subclasses is based on literature review (Agarwal et al. 2013; Jhariya et al. 2016; Murmu et al. 2019), opinions of hydrogeology experts (who have a deep understanding of the region's groundwater tables), and field knowledge, using the 1 to 9 Saaty scale (Saaty 2004, 2008).

After comparing each layer based on their relative importance, a pairwise comparison matrix for the nine variables (in this case, DEM, slope, drainage density, lineament density, LULC, geology, lithology, vegetation cover, and rainfall) is constructed (Table 2). To calculate

the normalized weights, the sum of values for each column is estimated using Equation (6) and shown at the bottom of the table.

$$L_{ij} = \sum_{n=1}^n C_{ij} \tag{6}$$

Here, L_{ij} is the sum of values for each column of the pairwise comparison matrix, and C_{ij} is the variable used for analysis.

In AHP analysis, a comparison of the considered criteria in terms of number (n) must be performed, and a square matrix of $A = (a_{ij})$ is created. For this purpose, all values of each column are divided by the sum of that column through Eq. (7) to create a normalized pairwise comparison matrix. The normalized weight (N wt) of each variable is obtained by averaging all values for each row of the normalized pairwise comparison matrix (Table 3). The sum of normalized weights is always one. The highest weight, similar to the study by (Mallick et al. 2019), was attributed to lithology, and the lowest weight was allocated to the rainfall variable.

$$A = \begin{bmatrix} a_{11} & a_{21} & \dots & a_{1n} \\ a_{21} & a_{22} & \dots & a_{2n} \\ \vdots & \vdots & & \vdots \\ a_{n1} & a_{n2} & \dots & a_{nm} \end{bmatrix} a_{ij} = \frac{a_{ij}}{\sum_1 a_{ij}} i, j = 1, 2, \dots, n \tag{7}$$

During the application of the AHP method, a certain level of inconsistency may arise from subjective or mental judgments. To assess accuracy, the consistency ratio (CR) must be calculated. To this end, the statistics of eigenvalue and eigenvector were calculated from Eqs. (8) and (9), respectively, for the weights assigned to the nine thematic layers and their subclasses. First, each column of the pairwise comparison matrix is multiplied by the weight of the corresponding variable. Then, the average weight value is obtained through the sum of rows. Dividing the

Table 2 Pairwise comparison matrix of the nine variables for AHP method

Variable	Lithology	Geology	DD	Slope	DEM	NDVI	LD	LULC	Rainfall
Lithology	1	2	3	4	5	6	7	8	9
Geology	0.500	1	3	4	5	6	7	8	9
DD*	0.333	0.333	1	2	2	6	7	8	9
Slope	0.250	0.250	0.500	1	2	5	8	7	9
DEM	0.200	0.200	0.500	0.500	1	5	5	8	9
NDVI	0.166	0.166	0.166	0.200	0.200	1	2	5	7
LD*	0.143	0.143	0.143	0.166	0.143	0.333	1	2	3
LULC*	0.125	0.125	0.125	0.143	0.125	0.200	0.500	1	3
Rainfall	0.111	0.111	0.111	0.111	0.111	0.143	0.333	0.333	1
SUM	2.828	4.328	8.545	12.121	15.578	29.676	38.833	47.333	59

LULC Land use and land cover, LD lineament density, DD drainage density

Table 3 Normalized pairwise comparison matrix of the nine variables using the AHP method

Variable	Lithology	Geology	DD	Slope	DEM	NDVI	LD	LULC	Rainfall	Total	Nwt
Lithology	0.354	0.462	0.351	0.33	0.321	0.202	0.18	0.169	0.153	2.522	0.28
Geology	0.176	0.231	0.351	0.33	0.322	0.202	0.18	0.169	0.152	2.114	0.23
DD*	0.118	0.077	0.117	0.165	0.128	0.202	0.18	0.169	0.153	1.309	0.15
Slope	0.088	0.057	0.059	0.083	0.128	0.168	0.155	0.148	0.152	1.039	0.12
DEM	0.071	0.046	0.057	0.041	0.064	0.168	0.18	0.169	0.153	0.951	0.11
NDVI	0.059	0.039	0.02	0.016	0.013	0.034	0.077	0.106	0.119	0.482	0.05
LD*	0.051	0.033	0.017	0.014	0.009	0.011	0.026	0.042	0.051	0.253	0.03
LULC*	0.044	0.029	0.015	0.012	0.008	0.008	0.013	0.021	0.051	0.199	0.02
Rainfall	0.039	0.026	0.013	0.009	0.007	0.005	0.009	0.007	0.016	0.132	0.01

LULC Land use and land cover, LD lineament density, DD drainage density

total weight value by the weight of each variable gives the value of (λ). The maximum eigenvalue (λ_{max}) is calculated through Eq. (9), which is 10.1 in this case.

$$A = \begin{bmatrix} w_1 \\ w_2 \\ \vdots \\ w_n \end{bmatrix} \text{ and } w_i = \frac{\sum_1^n a_{ij}}{n} \text{ for } i = 1, 2, \dots, n \quad w' = AW = \begin{bmatrix} w'_1 \\ w'_2 \\ \vdots \\ w'_n \end{bmatrix} \tag{8}$$

$$\left(\lambda_{max} = \frac{1}{n} \left(\frac{w'_1}{w_1} + \frac{w'_2}{w_2} + \dots + \frac{w'_n}{w_n} \right) \right) \tag{9}$$

Here, W is the eigenvector, a is the eigenvalue of criterion i , and λ_{max} is the eigenvalue of the pairwise comparison matrix.

After that, the uncertainty judgment is obtained based on Saaty's consistency index (CI), calculated through Equation (10). The CI value in this work is 0.13.

$$CI = \frac{\lambda_{max} - n}{n - 1} \tag{10}$$

Here, n represents the number of criteria or subclasses.

Finally, the consistency ratio (CR) is obtained by dividing the consistency index by the random index (RI). The consistency ratio (CR) of a pairwise matrix is calculated through Eq. (11):

$$CR = \frac{CI}{RI} \tag{11}$$

Here, RI is the random index. RI values represent different numbers from n , as shown in Table 4.

The CR value must be less than or equal to 0.1 (Maity and Mandal 2019). Otherwise, if the consistency ratio is equal to or greater than 0.1, a review of judgments must be undertaken.

Otherwise, the AHP analysis may produce flawed results (Chakraborty and Banik 2006). Considering the nine variables and referring to Table 3, the value of the random index or RI is 1.45. Therefore, the consistency ratio in this case is 0.094, indicating acceptable inconsistency.

Weighted Overlay Analysis

After internal weighting of each thematic layer and prioritizing modeling criteria relative to the integration of selected thematic maps for the preparation of GWPZs, Equation (12) was applied in a GIS environment.

$$GWPZ = \sum_{j=1}^m \sum_{i=1}^n (w_j * w_i) \tag{12}$$

Here, w_i and w_j are the normalized weights of the i th and j th classes of thematic layers, respectively. m represents the total number of thematic layers, and n denotes the total number of subclasses in each thematic layer. Finally, higher values resulting from this equation indicate greater potential for the presence of groundwater (Malczewsk 1999; Agarwal and Garg 2016).

Step 4: validation and mapping of potential groundwater zones

At the end of the study, the predicted potential groundwater zones are validated in relation to the data collected from the existing exploitation wells (485 active wells) in the region. The analysis of the ROC curve is a standard technique for assessing the accuracy of a diagnostic test. The ROC curve plots false positive rates (FPR) on the horizontal axis (X-axis) and true positive rates (TPR) on the vertical axis (Y-axis) (Pradhan 2013). The area under the curve (AUC) of the ROC indicates the accuracy of a prediction process by explaining the system's

Table 4 Saaty's random index (RI) for different values of n

n	1	2	3	4	5	6	7	8	9	10
RI	0.00	0.00	0.52	0.90	1.12	1.24	1.32	1.41	1.45	1.45

ability to anticipate the precise occurrence or non-occurrence of predefined events. A curve with the largest AUC represents the best method.

Naghibi et al. (2015) summarized the relationship between the AUC and the accuracy of prediction as follows: excellent (0.9 to 1), very good (0.8 to 0.9), good (0.7 to 0.8), average (0.6 to 0.7), and poor (0.5 to 0.6). This curve is generated by plotting the TPR, also known as the sensitivity, against FPR, also known as 1-specificity. In conventional methodology, the FPR and TPR are displayed on the respective axes (Equations 13 and 14).

$$X = \text{FPR} = 1 - \frac{\text{TN}}{\text{TN} + \text{FP}} \quad (13)$$

$$Y = \text{TPR} = \frac{\text{TP}}{\text{TP} + \text{FN}} \quad (14)$$

The AUC of the ROC chart is used as a metric to measure the accuracy of the model's predictions. This chart assesses the comparison between the performance in terms of false positive percentage and true positive percentage. The true positive percentage indicates instances where the expected yield from the prediction map matches the actual yield. On the other hand, the false positive percentage represents the percentage of incorrectly diagnosed positive cases.

Results and discussion

The analytical process applied in this study culminated in insightful findings regarding the groundwater potential in the Goharkooh Plain. Subsequent to the weight assessment conducted using the AHP, each thematic raster layer underwent standardization and reclassification. Aligning with the methodologies employed in recent studies, such as those by (Ndhlovu and Woyessa 2021; Khan et al. 2022), a ranking value system ranging from 1 to 5 was adopted. These rankings correspond to very low, low, moderate, high, and very high categories for each thematic layer, respectively. Table 5 presents the normalized weights assigned to each thematic layer and the normalized ranks allocated to each subclass within these layers. As per the data in the table, the lithology layer was assigned the highest weight (0.28), while the rainfall layer was designated the lowest weight (0.01). Weights for the internal subclasses of each layer varied between 0.33 and 0.07, reflective of their respective direct or inverse correlations with groundwater permeability and recharge capacities.

Spatial distribution of thematic layers

Lithology

Utilizing the AHP, it was determined that the lithology thematic layer holds a substantial weight of 28% (as shown in Table 5), rendering it the most significant factor influencing groundwater potential in the study area. Given the direct correlation between lithology and permeability, classes exhibiting higher permeability were assigned elevated ranks, and conversely for less permeable classes. This led to the reclassification of the lithology thematic layer into five distinct groups, thereby generating a revised lithology layer reflective of varying permeability levels. This layer's highest ranking (Class 5) was attributed to the Quaternary (Q) sedimentary deposits, as depicted in Fig. 6A.

Geology

The study revealed that lithologies from the Pliocene, Miocene, and Eocene geological epochs, often composed of conglomerates, exhibit good to moderate permeability. Conversely, lithologies dating back to the Paleocene, Cretaceous, Oligocene, and Permian epochs, characterized frequently by a composition of rich mixtures and hard rocks, demonstrate poor permeability, as supported by (Mallick et al. 2019). Consequently, the geology (age) thematic layer was assigned a substantial weight of 23% (refer to Table 5). Within this layer, the subclasses—namely Quaternary and Pliocene, Miocene, Eocene, Paleocene, and the combined group of Cretaceous, Oligocene, and Permian—were ranked on a scale from very good to very poor, corresponding to numerical values ranging from 5 to 1, as illustrated in Fig. 6B.

Drainage density

Within the Goharkooh watershed, the drainage density thematic layer was ascribed a significant weight of 15% (as indicated in Table 5), positioning it as the region's third most influential factor for groundwater potential. Owing to the inverse relationship between drainage density and surface water accumulation, areas with lower drainage densities were assigned higher ranks. Accordingly, the subclasses within this layer, categorized as (0–2), (2–4), (4–6), (6–8), and (8–10), were ranked on a scale from very good to very poor. This ranking system corresponds to numerical values ranging from 5 to 1, as depicted in Fig. 6C.

Table 5 Normalized weights and ranks assigned for thematic layers and subclasses

Theme	Normalized layer weight	Class	Class rank	Normalized class rank
Lithology	0.28	Q	5	0.33
		PIQ, Qbl, Qa2	4	0.27
		Msc, Efs	3	0.20
		Es/sh, Qan	2	0.13
		Db, gb, gd, Jk, Ple, Pm, Cm, Efv	1	0.07
Geology (AGE)	0.23	Quaternary, Pliocene	5	0.33
		Miocene	4	0.27
		Eocene	3	0.20
		Paleocene	2	0.13
		Cretaceous, Oligocene, Permian	1	0.07
Drainage Density (km/km ²)	0.15	0–2	5	0.33
		2–4	4	0.27
		4–6	3	0.20
		6–8	2	0.13
		8–10	1	0.07
Slope Gradient (degree)	0.12	0–3	5	0.33
		3–5	4	0.27
		5–8	3	0.20
		8–10	2	0.13
		> 10	1	0.07
DEM (m)	0.11	1200–1250	5	0.33
		1250–1300	4	0.27
		1300–1400	3	0.20
		1400–1600	2	0.13
		> 1600	1	0.07
NDVI	0.05	–0.17–0.14	1	0.07
		0.14–0.18	2	0.13
		0.18–0.27	3	0.20
		0.27–0.36	4	0.27
		0.36–0.45	5	0.33
Lineament Density (km/km ²)	0.03	0–0.2	1	0.07
		0.2–0.4	2	0.13
		0.4–0.6	3	0.20
		0.06–0.8	4	0.27
		0.8–1.2	5	0.33
LU/LC	0.02	Cultivated land, Fallow land	5	0.33
		Bushland, Rich pastures	4	0.27
		Moderate pastures, Tree	3	0.20
		Poor pasture, Low density forest	2	0.13
		Settlement, Outcrop	1	0.07
Annual rainfall (mm)	0.01	92–95	1	0.07
		95–100	2	0.13
		100–110	3	0.20
		110–120	4	0.27
		120–140	5	0.33

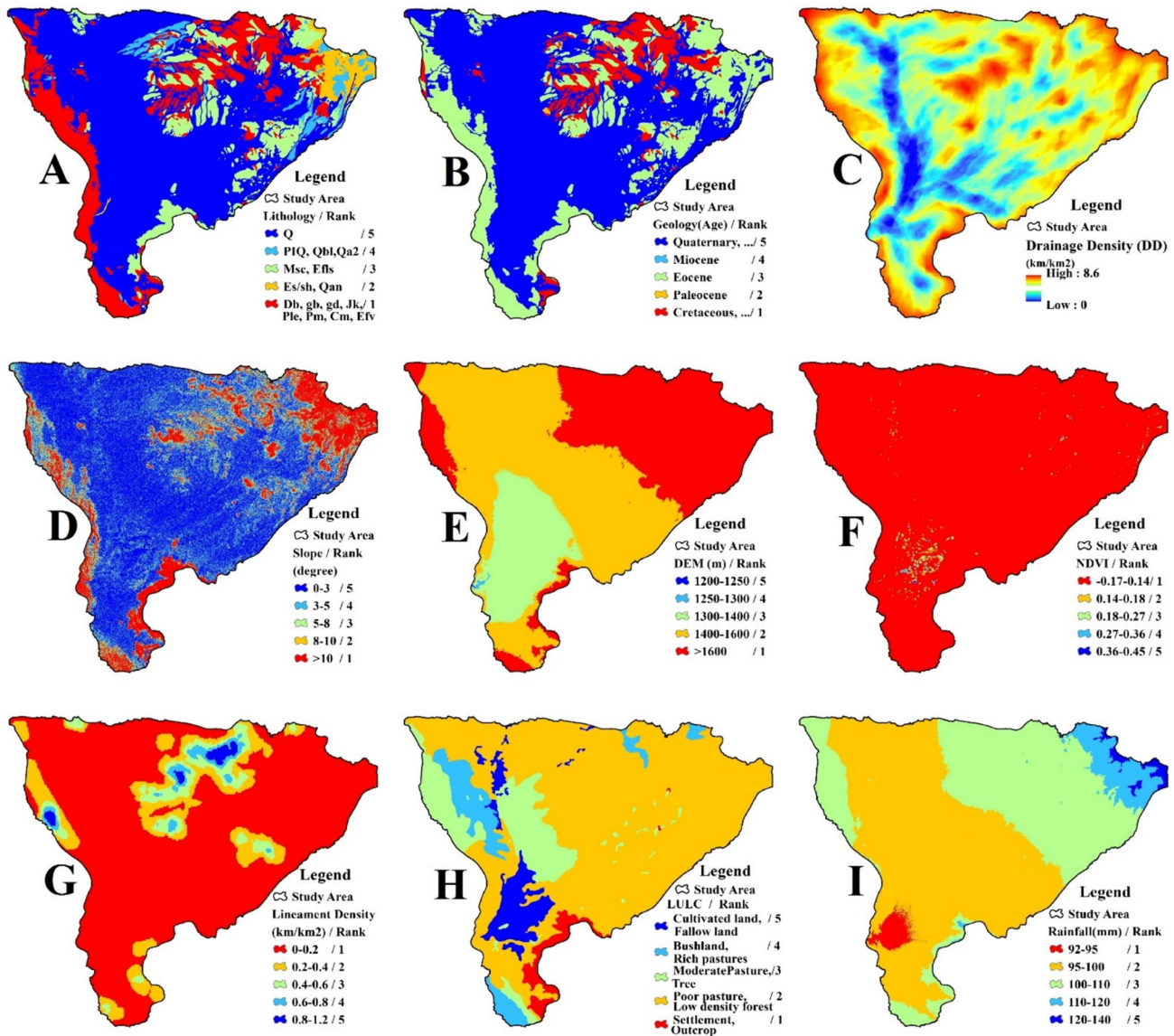


Fig. 6 Reclassify maps of: **A** lithology; **B** geology; **C** drainage density; **D** slope; **E** DEM; **F** NDVI; **G** lineament density; **H** LULC; and **I** rainfall

Slope gradient

In assessing the Goharkooh watershed, the slope gradient thematic layer was allocated a weight of 12% (refer to Table 5), marking it as the fourth most significant factor influencing groundwater potential. Given the inverse relationship between slope gradient and surface water accumulation, areas with gentler slopes received higher rankings. Consequently, the subclasses within this layer, defined as (0–3), (3–2), (3–5), (5–8), and (8–10), were assigned ranks from very good to very poor. This ranking corresponds to a numerical range from 5 to 1, as illustrated in Fig. 6D.

DEM

The DEM thematic layer has been identified as the fifth most critical factor affecting groundwater potential in the Goharkooh watershed, with an assigned weight of 11% as per Table 5. According to Arulbalaji et al. (2019), there exists an inverse correlation between surface water accumulation, drainage density, and DEM and a direct correlation with slope (Arulbalaji et al. 2019). This relationship necessitates assigning higher weights to lower elevations and lower weights to higher elevations. Accordingly, the subclasses within this layer, categorized as (1200–1250), (1250–1300), (1300–1400), (1400–1600), and (> 1600), have been ranked from very good to very poor. These

rankings correspond to a numerical range from 5 to 1, as depicted in Fig. 6E.

Vegetation cover

The vegetation covers the thematic layer, ranking sixth, received a weight of 5% (Table 5). The NDVI was used to categorize vegetation density into five subclasses. These subclasses range from very poor potential, corresponding to a very low NDVI range, to very high potential, associated with a high NDVI range. This classification is denoted by a numerical range of 1 to 5, as shown in Fig. 6F. Notably, most of the study area is classified with a very low rank in terms of vegetation cover.

Lineament density

The lineament density thematic layer was assigned a weight of 3% in the groundwater potential of the study area (Table 5). The reclassified lineament density map delineates the area into five distinct classes, as depicted in Fig. 6G. These classes range from high potential, corresponding to very high lineament density, to very low potential, associated with very low lineament density. The rankings for these classes span from 5 to 1, with higher-density subclasses receiving higher ranks. Consequently, the subclasses (0.8–1.09), (0.6–0.8), (0.4–0.6), (0.2–0.4), and (0–0.2) are, respectively, assigned ranks from very good to very poor.

LULC

In the overall assessment of groundwater potential for the Goharkooh watershed, the LULC criterion has been assigned a weight of 2%, as indicated in Table 5. Subsequently, the reclassified LULC map categorizes the area into five distinct classes. These classes are arranged according to the potential for water infiltration, ranging from very high to very low potential. The ranking system for these classes is denoted by numerical values from 5 to 1, as illustrated in Fig. 6H.

Precipitation

The weighting and grading of annual precipitation amounts are based on the method by (Khan et al. 2022), where higher weights are assigned to higher precipitation amounts and vice versa (Fig. 6I). The spatial distribution layer of total annual precipitation in the Goharkooh watershed, with a weight of 1% (Table 5), has the least contribution to groundwater potential assessment. However, as noted by researchers such as (Uc Castillo et al. 2022) and (Abdullateef et al. 2021), rainfall is the main hydrological source of groundwater recharge in semiarid regions.

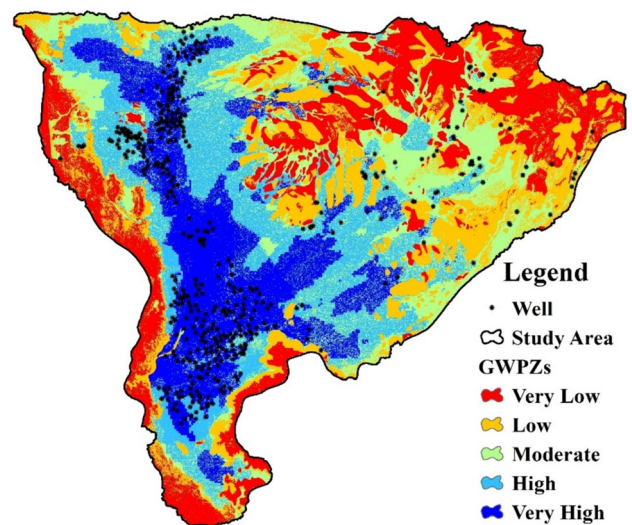


Fig. 7 GWPZs in the Goharkooh basin

Table 6 Area and percentage of GWPZs in the Goharkooh basin

Categories	Area (km ²)	Area (%)
Excellent	550	19.98%
Good	563	20.45%
Moderate	556	20.19%
Poor	574	20.85%
Very Poor	510	18.53%
Total	2753	100%

GWPZs

A weighted overlay analysis was conducted to delineate GWPZs, incorporating the relative significance of various thematic layers and their respective subclasses. During the overlay analysis, the weight assigned to each thematic layer is multiplied by the rank of its subclasses, subsequently integrating these products across all layers. The specific weights of the thematic layers and their subclasses are detailed in Table 5. The groundwater potential index (GWPI), derived from Eq. (12), is presented in the groundwater potential zoning map (Fig. 7). This aggregation of the nine influential factors results in the classification of the GWPZs into five distinct categories: very good, good, moderate, poor, and very poor potential. The 'very good' potential zone is characterized by favorable lithological and geological conditions, coupled with low drainage density and gentle slopes, which enhance infiltration capabilities, particularly in the flat and downstream segments of the basin. Table 6, which presents the area percentages for each groundwater potential class, indicates that this zone constitutes approximately 20% of the total study area.

Zones with very good and good groundwater potential, covering about 19.98% and 20.45% of the area, respectively, are located in geological formations of current alluvial deposits and conglomerates. These zones, characterized by geomorphological units of alluvial plains and alluvial fan plains, are further influenced by factors such as low drainage density, low slope and elevation, vegetation cover density, and agricultural land use. These conditions provide ideal circumstances for water infiltration into the subsurface, thereby enhancing and developing groundwater resources. Conversely, the eastern areas of the basin, due to high drainage density influenced by high elevation and slope along with predominantly impermeable lithology, exhibit very poor groundwater potential, as indicated in Fig. 7. Similarly, the western peripheral areas of the study region display very poor groundwater potential due to the dominance of colorful mixture lithologies with low permeability. Collectively, zones with moderate, poor, and very poor potential comprise approximately 20.19%, 20.85%, and 18.53% of the Goharkooh watershed area, respectively. Overall, the study area predominantly exhibits very good, good, and moderate potential for groundwater, indicating a need for integrated water management strategies that address domestic water supply, environmental water needs, agriculture, and industry.

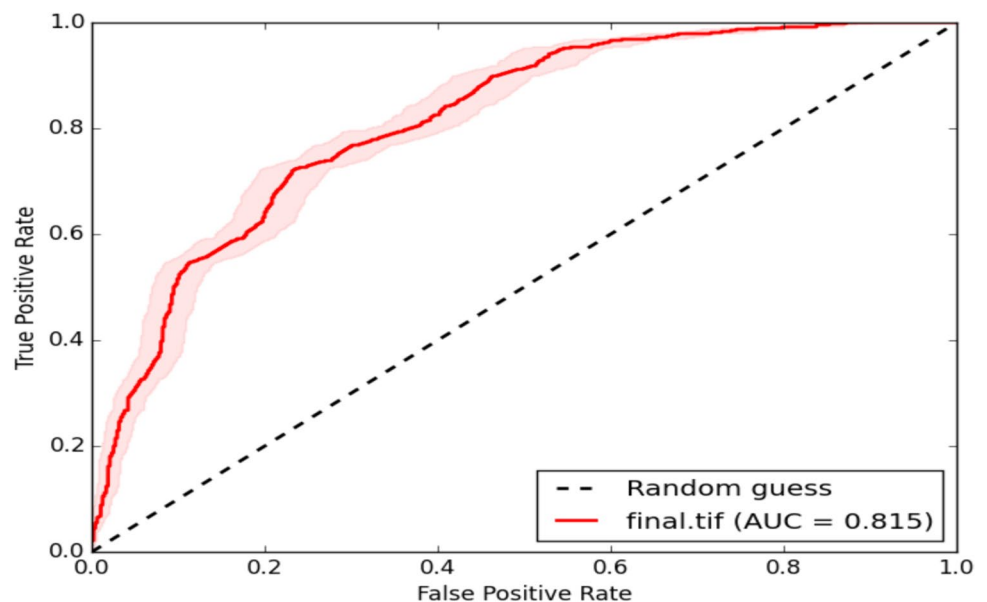
Validation of groundwater potential map

A dual-phase validation approach was implemented to evaluate the effectiveness of the groundwater potential zoning methodology developed in this study. The initial phase encompassed a visual comparison between the groundwater potential map and the spatial distribution of wells within the Goharkooh basin, as depicted in Fig. 7. This comparison

aimed to verify the reliability of the results obtained. A notable alignment between the distribution of existing wells and areas designated as having high groundwater potential suggested a commendable degree of accuracy in the generated map. This inference is based on the rationale that a higher concentration of productive wells serves as a robust indicator of significant groundwater availability in those zones. Of the 480 observation wells in the Goharkooh basin, 306 were in zones classified as having excellent potential, while 111 were located in areas deemed to have good potential. Additionally, the discharge rates of these wells were subject to scrutiny. Among the 393 wells with documented discharge rates, the minimum, maximum, and average discharge rates recorded were 0.3 L per second, 53 L per second, and 13.8 L per second, respectively. It was observed that 36% of these wells exhibited discharge rates surpassing the average, whereas 64% fell below the average. Wells with above-average discharge rates predominantly occurred in areas identified as having excellent potential, while those with lower rates were typically found in zones of good potential.

In applying the ROC curve method, AUC is an essential metric for assessing the model's accuracy, ranging from 0.5 to 1. In this study, a representative dataset was compiled by selecting random pixels from locations with and without wells. This dataset facilitated the evaluation of the model's capability to accurately predict groundwater potential areas, as shown in Fig. 8. The AUC value obtained for the applied methodology was 0.815, indicating a very good level of agreement, quantified at 81.5%, between the existing groundwater data and the identified potential groundwater zones. Such results underscore the efficacy of the weighted overlay analysis method as a reliable estimator of well performance and sensitivity within the Goharkooh watershed.

Fig. 8 Validation of the results of GWPZs



Conclusion

In this research, RS techniques, GIS, and MCDM were adeptly utilized in a structured four-stage process to assess GWPZs in the Goharkooh Plain, situated in the southeastern part of Iran's driest drainage basin, the Lut Desert. The process entailed comprehensive data collection, meticulous RS & GIS processing, the derivation of weights using the AHP, and an overlay analysis to identify GWPZs, culminating in model validation. The challenge posed by the scarcity of regional data on crucial thematic layers was addressed by strategically using satellite imagery and RS processing techniques. The application of the AHP method for criteria evaluation demonstrated that the nine selected factors—lithology, geology, drainage density, slope gradient, DEM, vegetation cover index, lineament density, LULC, and annual rainfall—contributed 28%, 23%, 15%, 12%, 11%, 5%, 3%, 2%, and 1%, respectively, to the groundwater potential modeling. A CR of 0.094 was achieved, indicating an acceptable degree of consistency in the expert judgments concerning the weights of these criteria and their subclasses in accordance with the AHP methodology.

The results of the weighted overlay index were classified into five distinct potential categories: very high, high, moderate, low, and very low. It was found that zones with very high groundwater potential, encompassing less than 20% of the study area, were primarily located in low-lying areas characterized by minimal drainage density and gentle slopes, particularly around recent alluvial deposits. This is further evidenced by the dense concentration of agricultural activities and significant exploitation of groundwater resources, as indicated by the high number of operational wells in these areas. Conversely, areas with high and moderate groundwater potential, constituting 20.45% and 20.19% of the basin area, exhibited a sparser distribution. These zones are generally situated on the peripheries of the very high potential areas and in the foothills, a pattern highlighted by the scattered rural settlements engaged in orcharding on the eastern slopes of the Goharkooh basin. The remaining zones, characterized by impermeable rock outcrops, steep terrain, sparse vegetation, and high drainage density, were identified as having poor to very poor groundwater potential. These areas, covering 20.85% and 18.53% of the basin area, respectively, are predominantly found in the eastern, central, and western edges of the watershed. A visual analysis of the spatial distribution of groundwater extraction wells within the basin revealed that 60% of the wells are located in the very high potential zone, with 20% in the high potential zone and the rest in other potential zones. The drilling of 40 wells deeper than 50 m, each with a discharge rate exceeding 20 L per second in areas of very high groundwater potential,

substantiates the accuracy of the groundwater potential mapping in the Goharkooh Plain. Additionally, the quantitative validation of the groundwater potential prediction map, employing the ROC curve with an AUC value of 0.815, corroborates the high predictive accuracy of the study.

This research offers substantial contributions to the effective management of groundwater resources. The delineation of zones according to their groundwater potential—ranging from very low to very high—paves the way for formulating targeted strategies to mitigate groundwater contamination and enhance resource management practices. Effective stewardship of existing underground aquifers and similar ecosystems is crucial to fulfill the water requirements of the target region in the foreseeable future, prevent further depletion of these vital resources, and promote sustainable development. The conceptual model employed in this study has proved to be adept at addressing the specific objectives of this research, demonstrating its efficacy and applicability in the field of groundwater management. Furthermore, considering the nearly equivalent significance and influence of certain criteria, such as geology and lithology, which exhibit identical spatial distributions, the integration of these layers is recommended as a potential avenue for future research.

Acknowledgements The authors would like to acknowledge the support of those who directly or indirectly contributed to the success of this study.

Author contributions H.N. was involved in conceptualization and investigation; H.N., M.S. and V.S. were responsible for methodology and writing—original draft preparation; H.N. and M.S. helped with software and validation; V.S. and M.M.R. contributed to formal analysis and writing—reviewing and editing; M.S. took part in visualization; and H.N. and M.M.R. participated in supervision. All authors have read and agreed to the published version of the manuscript.

Funding Open access funding provided by Széchenyi István University (SZE).

Data availability The data presented in this study are available upon corroborated request from the corresponding author.

Declarations

Conflict of interest The authors declare no conflict of interest.

Open Access This article is licensed under a Creative Commons Attribution 4.0 International License, which permits use, sharing, adaptation, distribution and reproduction in any medium or format, as long as you give appropriate credit to the original author(s) and the source, provide a link to the Creative Commons licence, and indicate if changes were made. The images or other third party material in this article are included in the article's Creative Commons licence, unless indicated otherwise in a credit line to the material. If material is not included in the article's Creative Commons licence and your intended use is not permitted by statutory regulation or exceeds the permitted use, you will need to obtain permission directly from the copyright holder. To view a copy of this licence, visit <http://creativecommons.org/licenses/by/4.0/>.

References

- Abdalla F (2012) Mapping of groundwater prospective zones using remote sensing and GIS techniques: a case study from the Central Eastern Desert. *Egypt J African Earth Sci* 70:8–17. <https://doi.org/10.1016/j.jafrearsci.2012.05.003>
- Abdullateef L, Tijani MN, Nuru NA et al (2021) Heliyon Assessment of groundwater recharge potential in a typical geological transition zone in Bauchi, NE-Nigeria using remote sensing / GIS and MCDA approaches. *Heliyon* 7:e06762. <https://doi.org/10.1016/j.heliyon.2021.e06762>
- Adham M, Jahan C, Mazumder Q et al (2010) Study on Groundwater recharge potentiality of Barind Tract, Rajshahi District, Bangladesh using GIS and remote sensing technique. *J Geol Soc India* 75:432–438
- Agarwal R, Garg PK (2016) Remote sensing and gis based groundwater potential & recharge zones mapping using multi-criteria decision making technique. *Water Resour Manag* 30:243–260. <https://doi.org/10.1007/s11269-015-1159-8>
- Agarwal E, Agarwal R, Garg RD, Garg PK (2013) Delineation of groundwater potential zone: An AHP/ANP approach. *J Earth Syst Sci* 122:887–898. <https://doi.org/10.1007/s12040-013-0309-8>
- Aghanabati A (2004) Geology of Iran: Tehran, Iran
- Akbar TA, Hassan QK, Ishaq S et al (2019) Investigative spatial distribution and modelling of existing and future urban land changes and its impact on urbanization and economy. *Remote Sens* 11:15. <https://doi.org/10.3390/rs11020105>
- Antonakos AK, Voudouris KS, Lambrakis NI (2014) Site selection for drinking-water pumping boreholes using a fuzzy spatial decision support system in the Korinthia prefecture, SE Greece. *Hydrogeol J* 22:1763–1776. <https://doi.org/10.1007/s10040-014-1166-5>
- Arulbalaji P, Padmalal D, Sreelash K (2019) GIS and AHP techniques based delineation of groundwater potential zones: a case study from southern Western Ghats, India. *Sci Rep* 9:1–17. <https://doi.org/10.1038/s41598-019-38567-x>
- Asgher MS, Kumar N, Kumari M et al (2022) Groundwater potential mapping of Tawi River basin of Jammu District, India, using geo-spatial techniques. *Environ Monit Assess* 194(240):1–21. <https://doi.org/10.1007/s10661-022-09841-9>
- Bagheri A, Hosseini S (2011) A system dynamics approach to assess water resources development scheme in the Mashhad plain, Iran, versus sustainability. In: *Proceedings of the 4th International Perspective on Water Resources & the Environment (IPWE)*. p 10
- Barik B, Ghosh S, Saheer Sahana A et al (2017) Water-food-energy nexus with changing agricultural scenarios in India during recent decades. *Hydrol Earth Syst Sci* 21:3041–3060. <https://doi.org/10.5194/hess-21-3041-2017>
- Bhave HD, Katpatal YB, Pophare AM (2019) Identification of groundwater recharge potential zones for a watershed using remote sensing and GIS. *Int J Adv Res Eng Technol* 10:121–135
- Brito TP, Bacellar LAP, Barbosa MSC, Barella CF (2020) Assessment of the groundwater favorability of fractured aquifers from the southeastern Brazil crystalline basement. *Hydrol Sci J* 65:442–454. <https://doi.org/10.1080/02626667.2019.1703993>
- Cay T, Uyan M (2013) Evaluation of reallocation criteria in land consolidation studies using the Analytic Hierarchy Process (AHP). *Land Use Policy* 30:541–548. <https://doi.org/10.1016/j.landusepol.2012.04.023>
- Chakraborty S, Banik D (2006) Design of a material handling equipment selection model using analytic hierarchy process. *Int J Adv Manuf Technol* 28:1237–1245. <https://doi.org/10.1007/s00170-004-2467-y>
- Chen W, Li H, Hou E et al (2018) GIS-based groundwater potential analysis using novel ensemble weights-of-evidence with logistic regression and functional tree models. *Sci Total Environ* 634:853–867. <https://doi.org/10.1016/j.scitotenv.2018.04.055>
- Dar IA, Sankar K, Dar MA (2010) Remote sensing technology and geographic information system modeling: An integrated approach towards the mapping of groundwater potential zones in Hardrock terrain, Mamundiyar basin. *J Hydrol* 394:285–295. <https://doi.org/10.1016/j.jhydrol.2010.08.022>
- Davoodi Moghaddam D, Rezaei M, Pourghasemi HR et al (2015) Groundwater spring potential mapping using bivariate statistical model and GIS in the Taleghan Watershed. *Iran Arab J Geosci* 8:913–929. <https://doi.org/10.1007/s12517-013-1161-5>
- Deepa S, Venkateswaran S, Ayyandurai R et al (2016) Groundwater recharge potential zones mapping in upper Manimuktha Sub basin Vellar river Tamil Nadu India using GIS and remote sensing techniques. *Model Earth Syst Environ* 2(137):1–13. <https://doi.org/10.1007/s40808-016-0192-9>
- Dinesh Kumar PK, Gopinath G, Seralathan P (2007) Application of remote sensing and GIS for the demarcation of groundwater potential zones of a river basin in Kerala, southwest coast of India. *Int J Remote Sens* 28:5583–5601. <https://doi.org/10.1080/0143160601086050>
- Elewa HH, Qaddah AA (2011) Groundwater potentiality mapping in the Sinai Peninsula, Egypt, using remote sensing and GIS-watershed-based modeling. *Hydrogeol J* 19:613–628. <https://doi.org/10.1007/s10040-011-0703-8>
- Feizizadeh B, Blaschke T (2012) Uncertainty analysis of GIS-based ordered weighted averaging method for landslide susceptibility mapping in Urmia Lake Basin, Iran. In: *7th International Geographic Information Science Conference*. p 5
- Foltz RC (2002) Iran's water crisis: cultural, political, and ethical dimensions. *J Agric Environ Ethics* 15:357–380
- Funk C, Verdin A, Michaelsen J et al (2015) A global satellite-assisted precipitation climatology. *Earth Syst Sci Data* 7:275–287. <https://doi.org/10.5194/essd-7-275-2015>
- Ghosh A, Adhikary PP, Bera B et al (2022) Assessment of groundwater potential zone using MCDA and AHP techniques: case study from a tropical river basin of India. *Appl Water Sci* 12(37):1–22. <https://doi.org/10.1007/s13201-021-01548-5>
- Golkarian A, Naghibi SA, Kalantar B, Pradhan B (2018) Groundwater potential mapping using C5.0, random forest, and multivariate adaptive regression spline models in GIS. *Environ Monit Assess* 190(149):1–16. <https://doi.org/10.1007/s10661-018-6507-8>
- Greenbaum D (1985) Review of remote sensing applications to groundwater exploration in basement and regolith
- Gupta M, Srivastava PK (2010) Integrating GIS and remote sensing for identification of groundwater potential zones in the hilly terrain of Pavagarh, Gujarat, India. *Water Int* 35:233–245. <https://doi.org/10.1080/02508061003664419>
- Haji Mohammadi M, Shafaie V, Nazari Samani A et al (2024) Assessing future hydrological variability in a semi-arid mediterranean basin: soil and water assessment tool model projections under shared socioeconomic pathways climate scenarios. *Water* 16(6):805
- Ifediegwu SI (2022) Assessment of groundwater potential zones using GIS and AHP techniques : a case study of the Lafia district, Nasarawa State. *Nigeria Appl Water Sci* 12(10):1–17. <https://doi.org/10.1007/s13201-021-01556-5>
- Izady A, Davary K, Alizadeh A et al (2012) Application of “ panel-data ” modeling to predict groundwater levels in the Neishaboor Plain. *Iran Hydrogeol J* 20:435–447. <https://doi.org/10.1007/s10040-011-0814-2>
- Jha MK, Chowdhury VM, Chowdhury A (2010) Groundwater assessment in Salboni Block, West Bengal (India) using remote sensing, geographical information system and multi-criteria decision analysis techniques. *Hydrogeol J* 18:1713–1728. <https://doi.org/10.1007/s10040-010-0631-z>

- Jhariya DC, Kumar T, Gobinath M et al (2016) Assessment of groundwater potential zone using remote sensing, GIS and multi criteria decision analysis techniques. *J Geol Soc India* 88:481–492
- Jhariya DC, Kumar T, Dewangan R et al (2017) Assessment of groundwater quality index for drinking purpose in the durg district, chhattisgarh using geographical information system (GIS) and multi-criteria decision analysis (MCDA) Techniques. *J Geol Soc India* 89:453–459
- Kaboli S, Hekmatzadeh AA, Darabi H, Haghighi AT (2021) Variation in physical characteristics of rainfall in Iran, determined using daily rainfall concentration index and monthly rainfall percentage index. *Theor Appl Climatol* 144:507–520. <https://doi.org/10.1007/s00704-021-03553-9>
- Kaewdum N, Chotpantarat S (2021) Mapping potential zones for groundwater recharge using a GIS technique in the lower Khwae hanuman sub-basin area, Prachin Buri province, Thailand. *Front Earth Sci* 9:1–16. <https://doi.org/10.3389/feart.2021.717313>
- Kamali Maskooni E, Naghibi SA, Hashemi H, Berndtsson R (2020) Application of advanced machine learning algorithms to assess groundwater potential using remote sensing-derived data. *Remote Sens* 12(2742):1–25. <https://doi.org/10.3390/rs12172742>
- Karra K, Kontgis C, Statman-Weil Z, et al (2021) Global land use / land cover with Sentinel 2 and deep learning. In: 2021 IEEE International Geoscience and Remote Sensing Symposium IGARSS. pp 4704–4707
- Khan R, Jhariya DC (2019) Assessment of groundwater pollution vulnerability using GIS based modified DRASTIC model in Raipur City, Chhattisgarh. *J Geol Soc India* 93:293–304. <https://doi.org/10.1007/s12594-019-1177-x>
- Khan MYA, Elkashouty M, Subyani AM et al (2022) GIS and RS intelligence in delineating the groundwater potential zones in Arid Regions : a case study of southern Aseer, southwestern Saudi Arabia. *Appl Water Sci* 12:1–23. <https://doi.org/10.1007/s13201-021-01535-w>
- Laurencelle J, Logan T, Gens R (2015) ASF Radiometrically Terrain Corrected ALOS PALSAR products. *Alaska Satell. Facil.* 1–12
- Leduc C, Favreau G, Schroeter P (2001) Long-term rise in a Sahelian water-table : the Continental Terminal in South-West Niger. *J Hydrol* 243:43–54
- Lee S, Song K, Kim Y, Park I (2012) Regional groundwater productivity potential mapping using a geographic information system (GIS) based artificial neural network model. *Hydrogeol J* 20:1511–1527. <https://doi.org/10.1007/s10040-012-0894-7>
- Li H, Lu Y, Zheng C et al (2019) Groundwater Level Prediction for the Arid Oasis of Northwest China Based on the Artificial Bee Colony Algorithm and a Back-propagation Neural Network with Double Hidden Layers. *Water* 11(860):1–20. <https://doi.org/10.3390/w11040860>
- Madani K (2014) Water management in Iran : what is causing the looming crisis ? *J Environ Stud Sci* 4:315–328. <https://doi.org/10.1007/s13412-014-0182-z>
- Magesh NS, Chandrasekar N, Soundranayagam JP (2012) Delineation of groundwater potential zones in Theni district, Tamil Nadu, using remote sensing, GIS and MIF techniques. *Geosci Front* 3:189–196. <https://doi.org/10.1016/j.gsf.2011.10.007>
- Maitty DK, Mandal S (2019) Identification of groundwater potential zones of the Kumari river basin, India: an RS & GIS based semi-quantitative approach. *Environ Dev Sustain* 21:1013–1034. <https://doi.org/10.1007/s10668-017-0072-0>
- Makonyo M, Msabi MM (2021) Identification of groundwater potential recharge zones using GIS-based multi-criteria decision analysis : a case study of semi-arid midlands Manyara fractured aquifer, North-Eastern Tanzania. *Remote Sens Appl Soc Environ* 23:100544. <https://doi.org/10.1016/j.rsase.2021.100544>
- Malczewsk J (1999) GIS and Multicriteria Decision Analysis. John Wiley and Sons Inc, New York, NY
- Mallick J, Khan RA, Ahmed M et al (2019) Modeling groundwater potential zone in a semi-arid region of Aseer using fuzzy-AHP and. *Water* 11(2656):1–29. <https://doi.org/10.3390/w11122656>
- Manap MA, Nampak H, Pradhan B et al (2014) Application of probabilistic-based frequency ratio model in groundwater potential mapping using remote sensing data and GIS. *Arab J Geosci* 7:711–724. <https://doi.org/10.1007/s12517-012-0795-z>
- Mukherjee P, Singh CK, Mukherjee S (2012) Delineation of groundwater potential zones in arid region of India — a remote sensing and GIS Approach. *Water Resour Manag* 26:2643–2672. <https://doi.org/10.1007/s11269-012-0038-9>
- Mumtaz R, Baig S, Kazmi SSA et al (2019) Delineation of groundwater prospective resources by exploiting geo-spatial decision-making techniques for the Kingdom of Saudi Arabia. *Neural Comput Appl* 31:5379–5399. <https://doi.org/10.1007/s00521-018-3370-z>
- Murmu P, Kumar M, Lal D et al (2019) Delineation of groundwater potential zones using geospatial techniques and analytical hierarchy process in Dumka district, Jharkhand. *India Groundw Sustain Dev* 9:100239. <https://doi.org/10.1016/j.gsd.2019.100239>
- Nag SK, Ghosh P (2013) Delineation of groundwater potential zone in Chhatna Block, Bankura District, West Bengal, India using remote sensing and GIS techniques. *Environ Earth Sci* 70:2115–2127. <https://doi.org/10.1007/s12665-012-1713-0>
- Naghibi SA, Pourghasemi HR, Pourtaghi ZS, Rezaei A (2015) Groundwater qanat potential mapping using frequency ratio and Shannon ' s entropy models in the Moghan watershed. *Iran Earth Sci Informatics* 8:171–186. <https://doi.org/10.1007/s12145-014-0145-7>
- Nampak H, Pradhan B, Manap MA (2014) Application of GIS based data driven evidential belief function model to predict groundwater potential zonation. *J Hydrol* 513:283–300. <https://doi.org/10.1016/j.jhydrol.2014.02.053>
- Ndhlovu GZ, Woyessa YE (2021) Integrated assessment of groundwater potential using geospatial techniques in Southern Africa : a case study in the Zambezi River Basin. *Water* 13(2610):1–20
- O'Leary DR, Izbicki JA, Moran JE et al (2012) Movement of water infiltrated from a recharge basin to wells. *Groundwater* 50:242–255. <https://doi.org/10.1111/j.1745-6584.2011.00838.x>
- Oh H, Kim Y, Choi J et al (2011) GIS mapping of regional probabilistic groundwater potential in the area of Pohang City, Korea. *J Hydrol* 399:158–172. <https://doi.org/10.1016/j.jhydrol.2010.12.027>
- Ozdemir A (2011) GIS-based groundwater spring potential mapping in the Sultan Mountains (Konya, Turkey) using frequency ratio, weights of evidence and logistic regression methods and their comparison. *J Hydrol* 411:290–308. <https://doi.org/10.1016/j.jhydrol.2011.10.010>
- Pourghasemi HR, Beheshtirad M (2015) Assessment of a data-driven evidential belief function model and GIS for groundwater potential mapping in the Koohrang Watershed. *Iran Geocarto Int* 30:662–685. <https://doi.org/10.1080/10106049.2014.966161>
- Pradhan B (2013) Computers & Geosciences A comparative study on the predictive ability of the decision tree, support vector machine and neuro-fuzzy models in landslide susceptibility mapping using GIS. *Comput Geosci* 51:350–365. <https://doi.org/10.1016/j.cageo.2012.08.023>
- Prasad P, Loveson VJ, Kotha M, Yadav R (2020) Application of machine learning techniques in groundwater potential mapping along the west coast of India. *Geoscience Remote Sens* 57:735–752. <https://doi.org/10.1080/15481603.2020.1794104>
- Rahman MM, Althobiani F, Shahid S et al (2022) GIS and remote sensing-based multi-criteria analysis for delineation of groundwater potential zones : a case study for industrial zones in Bangladesh. *Sustainability* 14(6667):1–25. <https://doi.org/10.3390/su14116667>
- Rahmati O, Nazari Samani A, Mahdavi M et al (2015) Groundwater potential mapping at Kurdistan region of Iran using analytic

- hierarchy process and GIS. *Arab J Geosci* 8:7059–7071. <https://doi.org/10.1007/s12517-014-1668-4>
- Rezaei M, Sargezi A (2010) Assessing the Effects of Artificial Recharge on the Goharkooh Plain Aquifer. *Sci Q J Geosci (In Persian)* 19:99–106
- Saaty TL (2004) Decision making—the analytic hierarchy and network processes (AHP/ANP). *J Syst Sci Syst Eng* 13:1–35
- Saaty TL (2008) Decision making with the analytic hierarchy process. *Int J Serv Sci* 1:83–98
- Safdari Z, Nahavandchi H, Joodaki G (2022) Estimation of Groundwater Depletion in Iran 's Catchments. *Water* 14(131):1–19. <https://doi.org/10.3390/w14010131>
- Sandoval JA, Tiburan CL Jr (2019) Identification of potential artificial groundwater recharge sites in Mount Makiling Forest Reserve, Philippines using GIS and Analytical Hierarchy Process. *Appl Geogr* 105:73–85. <https://doi.org/10.1016/j.apgeog.2019.01.010>
- Sapkota S, Pandey VP, Bhattarai U et al (2021) Groundwater potential assessment using an integrated AHP-driven geospatial and field exploration approach applied to a hard-rock aquifer Himalayan watershed. *J Hydrol Reg Stud* 37:100914. <https://doi.org/10.1016/j.ejrh.2021.100914>
- Scanlon BR, Keese KE, Flint AL et al (2006) Global synthesis of groundwater recharge in semiarid and arid regions. *Hydrol Process* 20:3335–3370. <https://doi.org/10.1002/hyp.6335>
- Selvam S, Manimaran G, Sivasubramanian P et al (2014) GIS-based Evaluation of Water Quality Index of groundwater resources around Tuticorin coastal city, south India. *Environ Earth Sci* 71:2847–2867. <https://doi.org/10.1007/s12665-013-2662-y>
- Selvam S, Dar FA, Magesh NS et al (2016) Application of remote sensing and GIS for delineating groundwater recharge potential zones of Kovilpatti Municipality, Tamil Nadu using IF technique. *Earth Sci Informatics* 9:137–150. <https://doi.org/10.1007/s12145-015-0242-2>
- Senanayake IP, Dissanayake DMDOK, Mayadunna BB, Weerasekera WL (2016) An approach to delineate groundwater recharge potential sites in Ambalantota, Sri Lanka using GIS techniques. *Geosci Front* 7:115–124. <https://doi.org/10.1016/j.gsf.2015.03.002>
- Shaban A, Khawlie M, Abdallah C (2006) Use of remote sensing and GIS to determine recharge potential zones : the case of Occidental Lebanon. *Hydrogeol J* 14:433–443. <https://doi.org/10.1007/s10040-005-0437-6>
- Singh LK, Jha MK, Chowdary VM (2018) Assessing the accuracy of GIS-based multi-criteria decision analysis approaches for mapping groundwater potential. *Ecol Indic* 91:24–37. <https://doi.org/10.1016/j.ecolind.2018.03.070>
- Souissi D, Msaddek MH, Zouhri L et al (2018) Mapping groundwater recharge potential zones in arid region using GIS and Landsat approaches, southeast Tunisia. *Hydrol Sci J* 63:1–18. <https://doi.org/10.1080/02626667.2017.1414383>
- Strahler AN (1957) Quantitative analysis of watershed geomorphology. *Trans Am Geophys Union* 38:913–920
- Tahmassebpour N, Rahmati O, Noormohamadi F, Lee S (2016) Spatial analysis of groundwater potential using weights-of-evidence and evidential belief function models and remote sensing. *Arab J Geosci* 9:1–18. <https://doi.org/10.1007/s12517-015-2166-z>
- Thapa R, Gupta S, Guin S, Kaur H (2017) Assessment of groundwater potential zones using multi-influencing factor (MIF) and GIS : a case study from Birbhum district, West Bengal. *Appl Water Sci* 7:4117–4131. <https://doi.org/10.1007/s13201-017-0571-z>
- Uc Castillo JL, Martínez Cruz DA, Ramos Leal JA et al (2022) Delineation of groundwater potential zones (GWPZs) in a semi-arid basin through remote sensing, GIS, and AHP approaches. *Water* 14(2138):1–29. <https://doi.org/10.3390/w14132138>
- Yeh HF, Lee C-H, Hsu K-C, Chang P-H (2009) GIS for the assessment of the groundwater recharge potential zone. *Environ Geol* 58:185–195. <https://doi.org/10.1007/s00254-008-1504-9>
- Yeh HF, Cheng Y, Lin H, Lee C (2016) Mapping groundwater recharge potential zone using a GIS approach in Hualian River. *Taiwan Sustain Environ Res* 26:33–43. <https://doi.org/10.1016/j.serj.2015.09.005>

Publisher's Note Springer Nature remains neutral with regard to jurisdictional claims in published maps and institutional affiliations.